

University of California - Davis

UCD-97-15
June, 1997

Maximizing Hadron Collider Sensitivity to Gauge-Mediated Supersymmetry Breaking Models

C.-H. Chen and J.F. Gunion

Department of Physics, University of California, Davis, CA, USA

Abstract

We consider typical hadron collider detector signals sensitive to delayed decays of the lightest neutralino to photon plus goldstino and demonstrate the potential for substantially increasing the portion of the general parameter space of a gauge-mediated supersymmetry breaking model that can be probed at the Tevatron.

It has been conventional [1, 2, 3, 4, 5] to analyze the sensitivity of the CDF and D0 experiments to supersymmetric models with gauge-mediated supersymmetry breaking [6] (GMSB models) under the assumption that the lightest neutralino decays promptly to a photon plus the goldstino. In this case, the hadron collider signal for supersymmetry would be events containing two or more isolated photons, deriving from decay of two or more neutralinos, plus missing energy (and possibly other particles). However, in the GMSB models for which explicit constructions are available, the neutralino decay is most naturally characterized by a substantial decay length, possibly of order tens to hundreds of meters. Events in which one or more of the neutralinos travels part way through the detector and then decays can be a substantial fraction of the total, as can events in which all the neutralinos exit the detector before decaying (the latter leading to the jets plus missing energy and other conventional signals for supersymmetry). In this Letter, we assess the increase in parameter space coverage at the Tevatron that results by combining the two-photon plus missing energy signal and the standard jets plus missing energy signal with a typical signature for a delayed neutralino decay within the detector. We find that the range of parameter space that can be probed is substantially increased for luminosities expected in Run II and at TeV33.

In the simpler GMSB models [6] the phenomenology is primarily determined by just two mass scales: the scale $\sqrt{\langle F \rangle}$ at which SUSY-breaking occurs and a scale $\Lambda \equiv \langle F_S \rangle / \langle S \rangle$ arising in the so-called messenger sector that communicates SUSY-breaking to the usual supersymmetric (sparticle) partners of the Standard Model (SM) particles. Here, $\langle F \rangle$ is the magnitude of the expectation value of a typical F -term component in the sector of the theory responsible for

supersymmetry breaking; F_S and S are the scalar and F -term components of the singlet superfield, \widehat{S} , member of the messenger sector. (In what follows, we will use F and F_S to denote $\langle F \rangle$ and $\langle F_S \rangle$.) A third mass scale is M , the mass-scale of the fermion members of the messenger sector. The scale \sqrt{F} determines the mass and couplings of the goldstone fermion, or goldstino (G), resulting from spontaneous SUSY-breaking [7, 8]. The scales Λ and M determine the soft-supersymmetry-breaking masses of the sfermions and gauginos.

For the $SU(3)$, $SU(2)$ and $U(1)$ gauginos,

$$M_i(M) = k_i N_m g \left(\frac{\Lambda}{M} \right) \frac{\alpha_i(M)}{4\pi} \Lambda, \quad (1)$$

where $k_3 = k_2 = 1$, $k_1 = 5/3$, respectively. For the squarks and sleptons

$$m_i^2(M) = 2\Lambda^2 N_m f \left(\frac{\Lambda}{M} \right) \left[c_3 \left(\frac{\alpha_3(M)}{4\pi} \right)^2 + c_2 \left(\frac{\alpha_2(M)}{4\pi} \right)^2 + \frac{5}{3} \left(\frac{Y}{2} \right)^2 \left(\frac{\alpha_1(M)}{4\pi} \right)^2 \right], \quad (2)$$

with $c_3 = 4/3$ (color triplets), $c_2 = 3/4$ (weak doublets), and $Y/2 = Q - T_3$. The integer N_m (which must be ≤ 4 to avoid Landau poles) depends upon the (model-dependent) matter content of the messenger sector. To avoid negative mass-squared for bosonic members of the messenger sector $M/\Lambda > 1$ is required; $M/\Lambda \geq 1.1$ is preferred to avoid fine-tuning, for which $f(\Lambda/M) \simeq 1$ and $1 \leq g(\Lambda/M) \leq 1.23$. For $M/\Lambda \geq 2$, $1 \leq g(\Lambda/M) \leq 1.045$. In this Letter, we will consider masses obtained with $g = f = 1$, for which Eqs. (1) and (2) imply $m_{\tilde{q}} : m_{\tilde{\ell}_L} : m_{\tilde{\ell}_R} : M_1 = 11.6 : 2.5 : 1.1 : \sqrt{N_m}$.

These results at scale M must be evolved down to the scale of the actual sparticle masses, denoted Q . The resulting gaugino masses are given by replacing $\alpha_i(M)$ in Eq. (1) by $\alpha_i(Q)$, a useful reference result being $\Lambda \sim (80 \text{ TeV}/N_m) (M_1/100 \text{ GeV})$. Evolution of the sfermion masses is detailed in Ref. [9]. Most important is the ratio

$$m_{\tilde{\ell}_R}/M_1 = \sqrt{6/5} \sqrt{r_1/N_m - (5/33)(1 - r_1)},$$

where $r_1 = (\alpha_1(M)/\alpha_1(Q))^2$. For the very broad range of $Q \geq m_Z$ and $M \leq 3 \times 10^6 \text{ TeV}$, $1 < r_1 \lesssim 1.5$, in which case the lightest of the sparticle partners of the SM particles is the \tilde{B} for $N_m = 1$ or the $\tilde{\ell}_R$ (more precisely, the $\tilde{\tau}_1$) for $N_m \geq 2$. Our numerical results are obtained by evolving from $M = 1.1\Lambda$. Aside from Λ , the only other free parameters of the model are then $\tan \beta$ and $\text{sign}(\mu)$ (which, combined with the known value of m_Z , fix the low-energy μ and B parameters describing Higgs superfield and scalar field mixing). For this study, we have taken $\tan \beta = 2$ and $\text{sign}(\mu) = -1$.

For the goldstino, one finds $m_G = F/(\sqrt{3}M_{\text{Planck}}) \sim 2.5 \left(\sqrt{F}/100 \text{ TeV} \right)^2 \text{ eV}$. In GMSB models, the small $\sqrt{F} \sim \mathcal{O}(100 - 1000 \text{ TeV})$ values envisioned imply that G will be the lightest supersymmetric particle. In this case, most early-universe scenarios lead to the requirement $m_G \lesssim 1 \text{ keV}$ (equivalent to $\sqrt{F} \lesssim 2000 \text{ TeV}$) to avoid overclosing the universe [10, 11]. The coupling of a sparticle to its SM partner plus the G is inversely proportional to F and is very weak for all F values of interest. As a result, all the sparticles other than the next-to-lightest

super particle (NLSP), *i.e.* the $\tilde{\chi}_1^0$ or $\tilde{\ell}_R$, undergo chain decay down to the NLSP. The NLSP finally decays to the G : *e.g.* $\tilde{B} \rightarrow \gamma G$ (and ZG if $M_{\tilde{B}} > m_Z$) or $\tilde{\ell}_R \rightarrow \ell G$. The $c\tau$ for NLSP decay depends on \sqrt{F} ; *e.g.* for $N_m = 1$

$$(c\tau)_{\tilde{\chi}_1^0 = \tilde{B} \rightarrow \gamma G} \sim 130 \left(\frac{100 \text{ GeV}}{M_{\tilde{B}}} \right)^5 \left(\frac{\sqrt{F}}{100 \text{ TeV}} \right)^4 \mu\text{m} \quad (3)$$

If $\sqrt{F} \sim 2000 \text{ TeV}$ (the upper limit from cosmology), then $c\tau \sim 21 \text{ m}$ for $M_{\tilde{B}} = 100 \text{ GeV}$; $\sqrt{F} \sim 100 \text{ TeV}$ implies a short but vertexable decay length. Thus, the signatures for GMSB models are crucially dependent on \sqrt{F} .

In the GMSB models [6], the SUSY-breaking sector lies at a higher mass scale than the messenger sector and SUSY-breaking is then communicated by a new strong interaction *at two-loops* to the messenger sector. The two-loop communication between the two sectors implies that $F/F_S \sim (16\pi^2/\alpha_m^2) \geq 2.5 \times 10^4$ for $g_m \leq 1$, where $\alpha_m = g_m^2/(4\pi)$ characterizes the strength of the gauge interactions responsible for the two-loop communication. The importance of F/F_S derives from the following inequality [12] (see also [11]): $(\sqrt{F}/2000 \text{ TeV}) \geq \sqrt{F/F_S} (m_{\tilde{\ell}_R}/100 \text{ GeV})/(27.5\sqrt{N_m})$.¹ For $m_{\tilde{\ell}_R} \geq 45 \text{ GeV}$ (the rough LEP limit) and the two-loop communication value of $F/F_S = 2.5 \times 10^4$, $\sqrt{F} \geq 5200 \text{ TeV}$ ($\sqrt{F} \geq 2600 \text{ TeV}$) for $N_m = 1$ ($N_m = 4$); *i.e.* even allowing for a factor of 2 or 3 uncertainty in the approximate lower bound, \sqrt{F} must lie near its upper limit from cosmology and the NLSP decay length will be long. Previous phenomenological analyses [1, 2, 3, 4, 5] have assumed that a model with $F/F_S \sim 1$ is possible,² in which case the rough bound becomes $\sqrt{F} \geq (73 \text{ TeV}/\sqrt{N_m})(m_{\tilde{\ell}_R}/100 \text{ GeV})$; *i.e.* \sqrt{F} could then be small, although nothing would prohibit \sqrt{F} values much larger than this lower limit. Thus, at the very least, it is highly relevant to assess how our ability to discover supersymmetry changes as a function of \sqrt{F} .

Motivated by the $ee\gamma\gamma$ event at the Tevatron [14], in this Letter we will focus on the ($N_m = 1$) scenario in which the $\tilde{\chi}_1^0$ (primarily \tilde{B}) is the NLSP. Phenomenology for the case in which \sqrt{F} is small and $\tilde{\chi}_1^0 \rightarrow \gamma + G$ decay is prompt has been studied [1, 2, 3, 4, 5]. The case where \sqrt{F} is very large and most $\tilde{\chi}_1^0$ decays occur outside the detector has not been examined; it is equivalent to conventional supersymmetry phenomenology with the constraints implied by Eqs. (1) and (2) among the sparticle masses. Phenomenology for intermediate \sqrt{F} values has also not been considered. Given the uncertainty in \sqrt{F} , it is appropriate to consider searching simultaneously for a set of signals that are sensitive to different \sqrt{F} values.

We focus on the D0 detector. Events were generated simultaneously for all SUSY production mechanisms by modifying ISASUGRA/ISAJET [19] to incorporate the GMSB boundary conditions, and then forcing delayed $\tilde{\chi}_1^0$ decays according to the predicted $c\tau$. We used the toy calorimeter simulation package ISAPLT. We simulated calorimetry covering $|\eta| \leq 4$ with a cell size given by $\Delta R \equiv \Delta\eta \times \Delta\phi = 0.1 \times 0.0875$ and took the hadronic (electromagnetic) calorimeter resolution to be $0.7/\sqrt{E}$ ($0.15/\sqrt{E}$). The D0 electromagnetic calorimeter was simplified to a thin cylinder with radius $r = 1 \text{ m}$ and length $-2 \leq z \leq +2 \text{ m}$. Also important to our

¹This inequality is valid to within a model-dependent factor of a few.

²To date, only one explicit model [13] purports to allow $F/F_S \sim 1$.

analysis will be the central outer hadronic D0 calorimeter (OHC), which we approximated as occupying a hollow solid cylinder defined by $-2 \leq z \leq +2\text{m}$ and radial region $2 \leq r \leq 2.5\text{m}$. It is important that the OHC is segmented into units of size $\Delta R \sim 0.1$ and that there are also several layers of inner hadronic calorimeter.

The signals are defined in terms of jets, isolated prompt photons and isolated photons emerging from $\tilde{\chi}_1^0$ decays occurring in the OHC (isolated OHC photons). A jet is defined by requiring $|\eta_{\text{jet}}| < 3.5$ and $E_T^{\text{jet}} > 25\text{ GeV}$ (for $\Delta R_{\text{coal.}} = 0.5$). A photon is a prompt photon candidate if it emerges immediately or from a $\tilde{\chi}_1^0$ decay that occurs before the $\tilde{\chi}_1^0$ has reached the electromagnetic calorimeter. The $(\eta_\gamma, \phi_\gamma)$ of such a photon is defined by the direction of the vector pointing from the interaction point to the point at which it hits the electromagnetic calorimeter. (This is generally not the same as the direction of the photon's momentum.) An isolated prompt photon is defined by requiring $|\eta_\gamma| < 1$ and $E_T^\gamma > 12\text{ GeV}$, with isolation specified by $E_T(\Delta R \leq 0.3) < 4\text{ GeV}$ (summing over all other particles in the cone surrounding the photon). Photons that emerge within the hollow cylinder defined by the electromagnetic calorimeter, but that are not isolated, are merged with hadronic jets as appropriate. An isolated OHC photon is defined as one that emerges from a $\tilde{\chi}_1^0 \rightarrow \gamma G$ decay that occurs within the body of the central OHC and has $E_T^\gamma > 15\text{ GeV}$, with isolation specified by $E_T(\Delta R \leq 0.5) < 5\text{ GeV}$ (summing over all other particles in the cone surrounding the location of the $\tilde{\chi}_1^0$ decay). For all signals, events are retained only if at least one of several sets of reasonable trigger requirements (too numerous to list here) are satisfied.

We consider three signals:

I: The standard SUSY signal of jets plus missing energy, dominant when the $c\tau$ for the $\tilde{\chi}_1^0$ is large. We employ D0 cuts [15]: (a) $n(\text{jets}) \geq 3$ — labelled $k = 1, 2, 3$ according to decreasing E_T ; (b) no isolated ($E_T^{\text{had.}}(\Delta R \leq 0.3) < 5\text{ GeV}$) leptons with $E_T > 15\text{ GeV}$; (c) $\cancel{E}_T > 75\text{ GeV}$; (d) $0.1 < \Delta\phi(\cancel{E}_T, j_k) < \pi - 0.1$ and $\sqrt{(\Delta\phi(\cancel{E}_T, j_1) - \pi)^2 + (\Delta\phi(\cancel{E}_T, j_2))^2} > 0.5$. The background cross section level has been estimated by D0 to be $\sigma_B = 2.35\text{ pb}$. The signal will be deemed observable if: (i) there are at least 5 signal events; (ii) $\sigma_S/\sigma_B > 0.2$; and (iii) $N_S/\sqrt{N_B} > 5$, where N_S and N_B are the numbers of signal and background events.

II: The prompt 2γ signal, dominant when $c\tau$ for the $\tilde{\chi}_1^0$ is small. Following Ref. [4], we require: (a) at least two isolated prompt photons (as defined above); and (b) $\cancel{E}_T > \cancel{E}_T^{\text{min}}$. Detection efficiency of 80% (100%) is assumed if $E_T^\gamma < 25\text{ GeV}$ ($> 25\text{ GeV}$). This signal should be completely free of background provided $\cancel{E}_T^{\text{min}}$ is adjusted appropriately as a function of luminosity. Based on the background results of [16] (see also [17]) and eye-ball extrapolations thereof, we estimate $\cancel{E}_T^{\text{min}} = 30, 50, 70\text{ GeV}$ is sufficient for $L = 100\text{ pb}^{-1}, 2\text{ fb}^{-1}, 30\text{ fb}^{-1}$, respectively. The signal will be deemed observable if there are 5 or more events.

III: A delayed γ appearance signal, useful for moderate to large $c\tau$ values. The best such signal is highly detector dependent. As already stated, we shall focus on signals associated with the outer hadronic calorimeter of the D0 detector. Consider an event in which a $\tilde{\chi}_1^0 \rightarrow \gamma G$ decay occurs inside one of the outer hadronic calorimeter (OHC) cells [18]. The γ will deposit all its energy in the cell. By demanding substantial γ energy and isolation (precise requirements were given earlier) for this deposit, along with other criteria, backgrounds can be made small.

³ More specifically, we require that the event fall into one of three classes defined by the following sets of requirements:

1. (a) $n(\text{jets}) \geq 3$; (b) at least one isolated OHC photon; (c) $\cancel{E}_T > \cancel{E}_T^{\min}$.
2. (a) any number of jets; (b) two or more isolated OHC photons; (c) $\cancel{E}_T > \cancel{E}_T^{\min}$.
3. (a) any number of jets; (b) at least one isolated prompt photon; (c) at least one isolated OHC photon; (d) $\cancel{E}_T > \cancel{E}_T^{\min}$.

In the absence of the needed detector-specific study, we have assumed zero background to 1.+2.+3. for the same $\cancel{E}_T^{\min} = 30, 50, 70 \text{ GeV}$ values at $L = 100 \text{ pb}^{-1}, 2 \text{ fb}^{-1}, 30 \text{ fb}^{-1}$ as employed for the prompt 2γ signal. Observability of the delayed-decay signals is assumed if the number of events for 1.+2.+3. is 5 or more.

The results of our analysis are displayed in Figs. 1, 2 and 3, for integrated luminosities $L = 100 \text{ pb}^{-1}, 2 \text{ fb}^{-1}$ and 30 fb^{-1} , respectively. For $L = 100 \text{ pb}^{-1}$, we observe that the prompt 2γ signal (+ points) allows SUSY detection out to $\Lambda \sim 55 \text{ TeV}$ (equivalent to $M_{\tilde{B}} \sim 70 \text{ GeV}$) so long as $\sqrt{F} \lesssim 400 \text{ TeV}$ (*i.e.* such that most $\tilde{\chi}_1^0$ decays are prompt). The standard jets plus \cancel{E}_T signature (\square points) is viable only for small $\Lambda \lesssim 26 \text{ TeV}$. The delayed $\tilde{\chi}_1^0$ decay signal(s) (\diamond points) expand the discovery region by only one scan point: $(\sqrt{F}, \Lambda) = (400 \text{ TeV}, 27 \text{ TeV})$. But, they are viable at some points where the previous two signals are observable and would then give an indication of the decay length of the $\tilde{\chi}_1^0$.

If D0 fails to observe the jets plus \cancel{E}_T signal in their current $L = 100 \text{ pb}^{-1}$ data then all the \square points in Fig. 1 will be excluded. Further, recent analyses by D0 [16] and CDF [17] place a 95% confidence level of less than 1 event on the prompt 2γ signal for essentially the same cuts and luminosity that we have considered here, which eliminates all the + points on this same plot. Thus, only if the stringent cuts we have employed for the delayed-decay signals could be weakened without encountering backgrounds would present data allow elimination of a significant additional portion of parameter space.

For $L = 2 \text{ fb}^{-1}$ (the nominal Run II integrated luminosity per detector), the parameter regions for which the prompt 2γ and delayed-decay signals are observable both expand dramatically. At moderate $\Lambda \lesssim 50 \text{ TeV}$, the delayed-decay signals probe out to larger \sqrt{F} than does the prompt 2γ signal, whereas for $\Lambda \gtrsim 30 \text{ TeV}$ only the prompt 2γ signal is viable for the smallest \sqrt{F} values. However, there are many points where both types of signal would be detectable. The region of viability for the standard jets + \cancel{E}_T signal expands only slightly to $\Lambda \lesssim 28 \text{ TeV}$.

For $L = 30 \text{ fb}^{-1}$ (the nominal TeV33 integrated luminosity per detector), the delayed-decay signals cover more of parameter space than either of the other two signals, with sensitivity out to $\sqrt{F} = 1400 \text{ TeV}$ for all Λ values explored. The region of overlap with the prompt 2γ

³Our additional criteria will be chosen so that the cross section for producing an isolated energetic long-lived kaon in association therewith is small. Further, any such kaon will interact strongly and is almost certain to be absorbed before reaching the OHC.

signal also expands significantly. The jets + \not{E}_T signature is still confined to relatively small $\Lambda \lesssim 28$ TeV values (for any \sqrt{F}).

Of the three delayed-decay signals, the first (≥ 3 jets + ≥ 1 OHC γ) is observable (*i.e.* yields at least five events) for *all* (Λ, \sqrt{F}) points where the delayed-decay signals are shown to be viable (the \diamond points in the figures). The second (≥ 2 OHC γ 's) yields ≥ 5 events for very few points. The third (≥ 1 prompt γ + ≥ 1 OHC γ) yields ≥ 5 events for the lower (roughly, half) \sqrt{F} portion of the \diamond regions of the figures. If simulations eventually show that the first signal is background-free for smaller \not{E}_T^{\min} than employed here (as we are hopeful will be the case), the portion of parameter space for which it is viable expands; *e.g.* at $L = 30 \text{ fb}^{-1}$ and $\not{E}_T^{\min} = 30 \text{ GeV}$ sensitivity would extend to $\sqrt{F} = 1800 \text{ TeV}$ for most of the Λ values shown.

We now briefly outline other possible delayed-decay signatures.

- Timing — Since the $\tilde{\chi}_1^0$ moves with v/c substantially less than 1, a late energy deposit would be a signal. In Run I, only CDF had any timing information for hadronic calorimeters, but some timing information will be available at both CDF and D0 for Run II [20].
- Impact parameter — If the impact parameter of a photon appearing in the electromagnetic calorimeter could be shown to be non-zero, this would also constitute a signal for a delayed decay. The extent to which the resolution for such an impact parameter measurement by the CDF and D0 detectors is adequate to establish a signal is under study. The LHC detectors have sufficiently better resolution that the non-zero impact parameter signal should be quite viable there.
- Timing and directional information outside the muon chambers — For large \sqrt{F} , many $\tilde{\chi}_1^0$ decays will occur outside the muon chambers. A multi-layer tracking array supplement to the cosmic ray veto would allow detection of such decays and provide a dramatic signal. Such an array would be useful for any delayed $\tilde{\chi}_1^0$ decay scenario.

Sensitivity to GMSB models with substantial $\tilde{\chi}_1^0$ decay length will be maximized by implementing all possible signals simultaneously. One can also envision construction of a special purpose detector for delayed decays [12]. One such proposal for the LHC has appeared [21].

If delayed decay signatures are seen, the next goal will be to determine the values of \sqrt{F} and Λ . The least model-dependent way of obtaining \sqrt{F} is to determine $c\tau$ and $m_{\tilde{\chi}_1^0}$ [see Eq. (3)]; $m_{\tilde{\chi}_1^0}$ then implies via Eq. (1) a value for Λ . To determine $c\tau$ requires knowledge of the distribution of $\tilde{\chi}_1^0$ decays. If both the prompt 2γ and OHC signals are seen, their relative rates will be a measure of $c\tau$. One way to measure $m_{\tilde{\chi}_1^0}$ would be to determine the time of flight to the OHC cell (requiring a measurement of the time of the OHC energy deposit) and correlate this with the energy of the deposit (*i.e.* the energy of the photon) which would reflect the energy of the decaying $\tilde{\chi}_1^0$. Substantial statistics will be required for both of these analyses.

In conclusion, we have argued that it is very natural (indeed, preferred in most existing models) for the general (Λ, \sqrt{F}) parameters of a gauge-mediated supersymmetry breaking model to be such that there is a large probability for the lightest neutralino to decay (to a photon plus goldstino) a substantial distance from the interaction point. We have shown that the portion of the parameter space for which a signal for supersymmetry can be seen at

the Tevatron is greatly expanded by employing signals sensitive to such delayed decays. The CDF and D0 detector groups should give detailed consideration to clarifying and refining such signatures.

Acknowledgments

This work was supported in part by the U.S. Department of Energy under grant No. DE-FG03-91ER40674, and by the Davis Institute for High Energy Physics. We are grateful to B. Dobrescu, S. Kuhlmann, S. Mani, H. Murayama, L. Nodulman, S. Thomas, A. White and A. Wicklund for helpful conversations.

References

- [1] S. Dimopoulos, M. Dine, S. Raby and S. Thomas, *Phys. Rev. Lett.* **76** (3494), 1996.
- [2] S. Ambrosanio, G. Kane, G. Kribs, S. Martin and S. Mrenna, *Phys. Rev. Lett.* **76** (3498), 1996.
- [3] S. Dimopoulos, S. Thomas and J.D. Wells, *Phys. Rev.* **D54** (3283), 1996.
- [4] H. Baer, M. Brhlik, C.-H. Chen and X. Tata, *Phys. Rev.* **D55** (4463), 1997.
- [5] J. Bagger, K. Matchev, D. Pierce and R.-J. Zhang, *Phys. Rev. Lett.* **78** (1002), 1997.
- [6] See, for example, M. Dine, A. Nelson and Y. Shirman, *Phys. Rev.* **D51** (1362), 1995; M. Dine, A. Nelson, Y. Nir and Y. Shirman, *Phys. Rev.* **D53** (2658), 1996; and references to earlier work therein.
- [7] P. Fayet, *Phys. Lett.* **B70** (461), 1977; *Phys. Lett.* **B86** (272), 1979; *Phys. Lett.* **B175** (471), 1986.
- [8] N. Cabibbo, G.R. Farrar and L. Maiani, *Phys. Lett.* **B105** (155), 1981; M.K. Gaillard, L. Hall and I. Hinchliffe, *Phys. Lett.* **B116** (279), 1982; J. Ellis and J.S. Hagelin, *Phys. Lett.* **B122** (303), 1983; D.A. Dicus, S. Nandi and J. Woodside, *Phys. Lett.* **B258** (231), 1991.
- [9] S. Martin, hep-ph/9608224.
- [10] H. Pagels and J.R. Primack, *Phys. Rev. Lett.* **48** (223), 1982; T. Moroi, H. Murayama and M. Yamaguchi, *Phys. Lett.* **B303** (289), 1993; S. Borgani, A. Masiero and M. Yamaguchi, *Phys. Lett.* **B386** (189), 1996.
- [11] A. de Gouvea, T. Moroi and H. Murayama, hep-ph/9701244.

- [12] J.F. Gunion, Proc. ITP Conference on Future High-Energy Colliders, Santa Barbara, CA, 21-25 Oct. 1996, hep-ph/9704349.
- [13] M. Luty, hep-ph/9706554.
- [14] S. Park (CDF Collaboration), “Search for New Phenomena in CDF”, 10th Topical Workshop on Proton–Antiproton Collider Physics, eds. R. Raja and J. Yoh, AIP Press, 1995.
- [15] S. Abachi *et al.* (D0 Collaboration), *Phys. Rev. Lett.* **75** (618), 1995.
- [16] S. Abachi *et al.* (D0 Collaboration), *Phys. Rev. Lett.* **78** (2070), 1997.
- [17] D. Toback (CDF Collaboration), FERMILAB-Conf-96/240-E.
- [18] The general idea of the OHC signal was developed in discussions with S. Mani.
- [19] F. Paige and S. Protopopescu, in *Supercollider Physics*, p. 41, ed. D. Soper (World Scientific, 1986); H. Baer, F. Paige, S. Protopopescu and X. Tata, hep-ph/9305342.
- [20] The rough detector features noted were gleaned from discussions with S. Kuhlmann (CDF), L. Nodulman (CDF), A.B. Wicklund (CDF), and S. Mani (D0).
- [21] K. Maki and S. Orito, hep-ph/9706382.

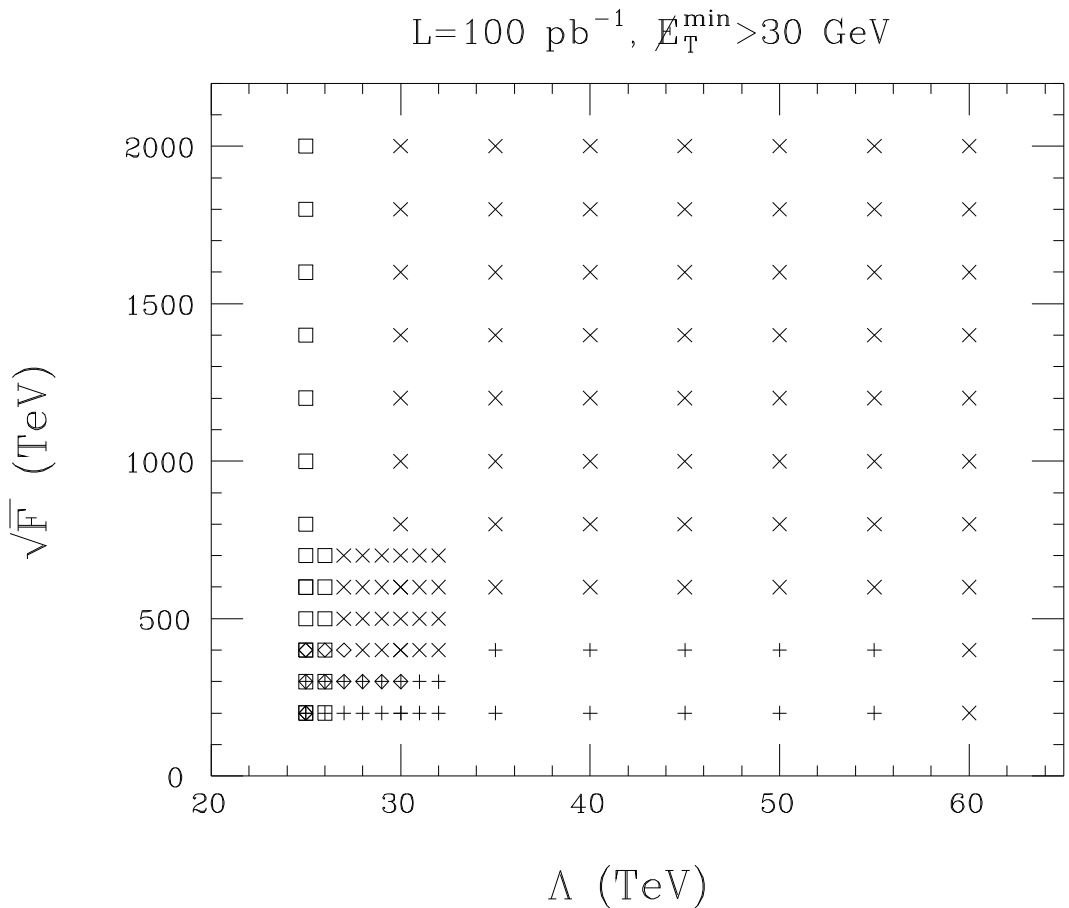


Figure 1: For $L = 100 \text{ pb}^{-1}$ and $\not{E}_T^{\min} = 30 \text{ GeV}$, we display those points in (Λ, \sqrt{F}) parameter space for which we can observe the following GMSB SUSY signals: \square , jets plus \not{E}_T ; $+$, prompt 2γ ; \diamond , OHC delayed-decay. At points labelled by \times , no signal is observable.

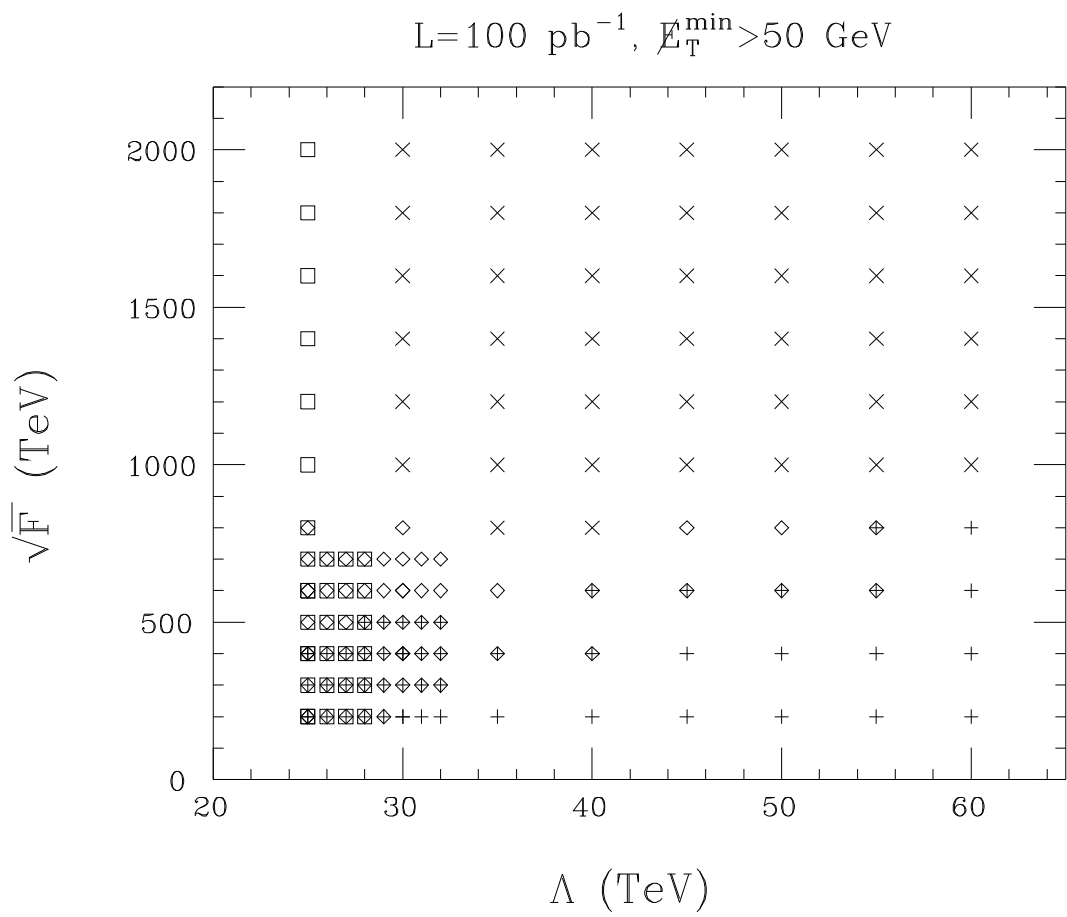


Figure 2: As in Fig. 1, but for $L = 2 \text{ fb}^{-1}$ and $\not{E}_T^{\min} = 50 \text{ GeV}$.

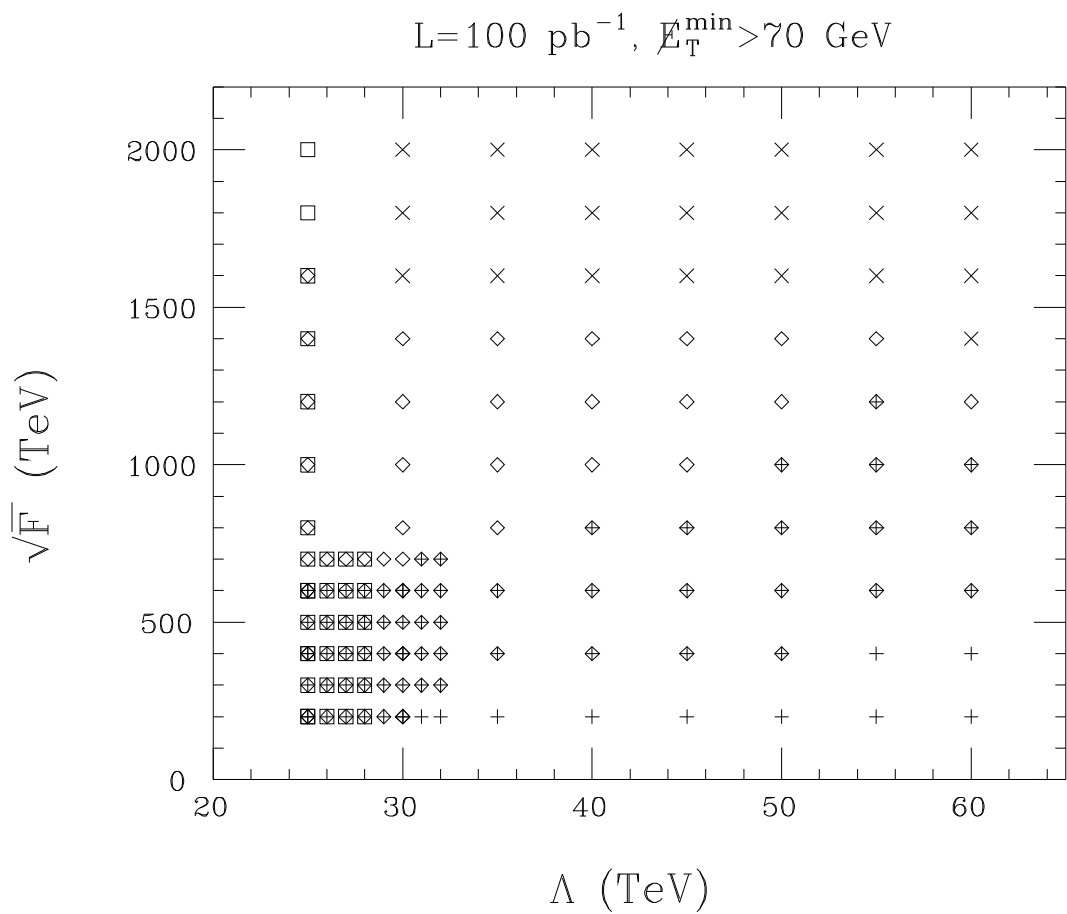


Figure 3: As in Fig. 1, but for $L = 30 \text{ fb}^{-1}$ and $\not{E}_T^{\min} = 70 \text{ GeV}$.